

Sensitivity study of the influence of the water boiling parameters on aluminum semi-continuous DC casting

Sébastien Bolduc¹, László I. Kiss¹

¹Université du Québec à Chicoutimi, Québec, Canada, G7H 2B1

Corresponding author : László I. Kiss¹, Laszlo_Kiss@uqac.ca

ABSTRACT

The thermal aspect is dominant in semi-continuous direct chill (DC) casting. In steady state, 80% of the total energy contained inside the ingot is evacuated by secondary cooling. For this reason, water is often suspected as a potential cause for the issues related to ingot quality. In the secondary cooling zone, the ingot is cooled by jet impingement boiling. Opinions in the literature about the influence of water quality on the boiling curve are conflicting. This can be associated mainly to the difficulties that experimenters meet during the measurement of the boiling curve repeatedly. Furthermore, published works present the entire boiling curve rather than identifying what are the significant parameters in it. This understanding is nonetheless essential in order to improve the measurement repeatability by focusing on the most significant boiling parameters as well as to ensure that the measured variations of the boiling curve are those that have an impact on the process. Considering this lack of knowledge, a sensitivity study has been completed to compare the relative influence of four parameters that characterize the boiling curve (Leidenfrost temperature, film boiling heat flux, critical heat flux and the temperature that belongs to the critical heat flux) on three issues responsible for the diminution of the recovery rate (hot tearing, bleed-out, butt curl). The study has shown that except the critical heat flux temperature, every tested boiling parameter plays a significant role on the three recovery rate obstacles. Moreover, for every case, a mutual interaction exists between the three significant boiling parameters. The latter demonstrates that the variation of each of the three most important boiling parameters is relevant and needs to be measured following a modification of the water quality. This study is the first step in the framework of a project aimed at the conception of an appropriate device for measuring the variation of the cooling capacity of water and its role on ingot quality.

Key words: aluminum, direct-chill casting, cooling water, impingement boiling, sensibility study

1. INTRODUCTION

The semi-continuous DC casting has been introduced in 1935 to produce large ingots for rolling, extrusion and forging. Numerous process modifications that improve the quality of ingots were subsequently published. The reader is referred to Eskin [1] for the history of process evolution since its invention.

Versatility, production rate, and good mechanical properties of the large aluminum ingots obtained by semi-continuous DC casting explain why the process has been in use for more than half a century. The aluminum alloy is first prepared inside a tilting furnace used to initiate a flow of liquid metal through launders mounted on top of the casting table. The casting molds allows the distribution of the cooling water towards a series of jets located at the bottom end of each casting mold. At start-up (figure 1a), a bottom block is used to retain the poured liquid aluminum inside the casting mold. A solidified shell is

subsequently formed due to the contact of the molten metal with the cooled surfaces of the casting mold (called primary cooling) and with the bottom block. The thermal energy contained in the middle of the ingot is then transported to the solidified shell by conduction and convection. The temperature difference inside the ingot thus forms a liquid aluminum pool called sump. When the thickness of the solidified shell is sufficient to withstand the hydrostatic pressure created by the sump depth, the bottom block starts a gradual descent allowing a direct cooling of the rolling and side faces by the water jets (figure 1b). The water discharged through the series of nozzles from the lower part of the mold is then used to cool the solidified shell by direct contact. The so-called secondary cooling is divided into two regions: (1) the impingement zone (10-15 mm) and (2) the free-falling zone (FFZ). The resulting high contraction rates at the rolling and side faces compared to interior of the ingot produce thermal stresses resulting in the lift off of the ingot from the bottom block causing the so-called butt curl. Optimization of process parameters is required to control the extent of the butt curl. The casting speed is increased progressively to a final constant value. Meanwhile, the temperature within the ingot varies as a function of time. During the transient regime, the sump depth and the isotherms within the ingot approach their steady state values and the permanent casting regime begins.

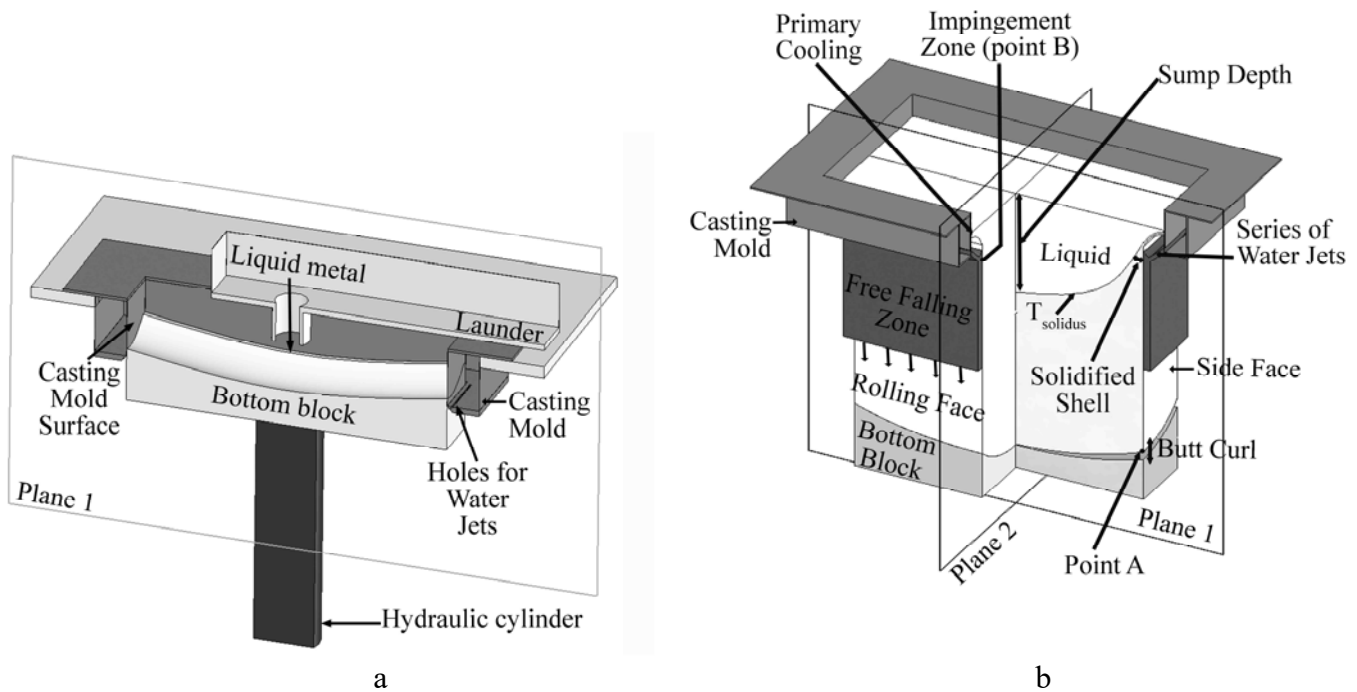


Figure 1 Scheme of aluminum DC casting at start-up (a); isometric view of water discharged from the lower part of the mold used to cool the aluminum ingot after start-up (b)

Considering its economic viability, the main challenge today remains the further improvement of the process for the reduction of production costs. When its quality does not meet customer requirements, the ingots are re-melted in a casting furnace that involves additional time and energy consumption. The percentage by mass of aluminum that does not need to be re-melted is used as performance indicator and is called recovery rate. Today's efforts concentrate on the improvement of the quality control of the ingot. During the last decade, the majority of research used numerical modeling to improve the existing process via better understanding [2]. For example, metal flow at the exit of the launder system, the role of the

cooling capacity of water and the optimization of materials used for casting molds were analyzed at the Aluminum Casthouse Technology Conference in 2009. [3]

Due to the large number of casting parameters (flow rate and temperature of water, casting speed, metal temperature, grain refinement), cast houses developed their own lists of settings called "casting recipes". The latter are often the result of a trial and error process [4] and differ according to ingot size and alloys. However, it was also found that for a given alloy and size the same casting recipe can lead to different results in terms of ingot quality. This indicates that the understanding of the process by the industry still needs to be improved.

The main ingot defects observed in the cast houses are well known. For each of these, there is a list of potential causes based on the current knowledge. Although the process involves a combination of hydrodynamic (flow of molten metal), heat transfer (water cooling) and mechanical stress (thermal contraction) mechanisms, the thermal aspect is dominant. In steady state, 80% of the total energy contained in the ingot [5] (superheat of the molten metal $\approx 5\%$, latent heat of solidification $\approx 35\%$ and the sensible heat of the solid metal $\approx 60\%$ [6]) is evacuated by secondary cooling (water jet and free-falling water) compared to only 20% within the mold (primary cooling zone). For this reason, water is often suspected as a potential cause for the issues related to the ingot quality.

At the impingement point, the water jets hit the solidified surface, which is at a temperature between 250 °C and 300 °C. [6] Since this temperature is much higher than the boiling point, bubble nucleation occurs at the surface but in most of the time the bubbles collapse rapidly inside the liquid film of water. This phenomenon is called jet impingement boiling on a vertical surface. The key characteristic of heat transfer by jet impingement boiling is the strong dependence of the heat flux on the surface temperature. According to the surface temperature, four boiling regimes exist. Nukiyama [7] was the first in 1934 to describe these regimes during pool boiling. He used a boiling curve to show the variation of the heat flux as function of the excess temperature above the boiling point. This curve is still used since to describe heat transfer during boiling.

The analysis of the influence of cooling water on the quality of ingots requires the measurement of the boiling curve. Two approaches exist: industrial [8-11] and laboratory measurements. Laboratory measurements can be obtained by quenching of a preheated cylindrical sample called "missile" [12-14] or by jet cooling of a larger preheated sample [15-19]. The industrial method involves the measurement of the cooling curve directly inside a real ingot during casting by thermocouples frozen into the cast metal. This is called the "freezing method" and has been proposed by Peel and Pengelly [8] in 1970. They measured the temperature variation near the surface inside a real cast ingot and computed the surface heat flux in order to adjust the heat transfer data used as boundary conditions.

The boiling curve can be described with a set of so-called boiling parameters that characterize its shape. Among the numerous variables that have an impact on the boiling curve, water quality is surely one of the most difficult to control. Water quality variations can be related to its chemical constitution, temperature or flow rate. The description of the impact of these variables on the boiling curve is conflicting in the literature [20]. For example, the effect of the same parameter is considered once as increasing, then as decreasing the heat flux for a given boiling regime. This situation occurs mainly because of the difficulties that experimenters confront in measuring the boiling curve reliably. For example, a literature review on the role of the critical heat flux (Q_{CHF}) by Li [21] reported variations between 1 and 5 MW/m² among the

different industrial measurements. Moreover, the best published repeatability obtained for measuring the Leidenfrost temperature (T_{leid}) in steady state is ± 7 °C [22]. Finally, quantifying the influence of a given parameter is complex since the parameters can be interrelated. In the latter case, a given parameter can promote bubble nucleation rate (increase Q_{CHF}) but decreasing T_{leid} which, in turn, increases the duration of the existence of a vapor film on the surface.

Based on literature review, it is important to identify the influence of each boiling parameter on the ingot quality before endeavouring to design a device for the reliable measurement of the boiling curve. In this way, only the parameters that have a significant influence on the process will be targeted and measured. For this reason, a sensitivity study was performed in the present study to clarify the importance of the different key parameters characterizing the boiling curve on the quality of cast ingots.

Although many finite element models exist currently, none has been used to compare the role of the characteristic parameters of the boiling curve in the development of defects observed in the ingots. The authors suggested this type of analysis for the first time in 2009 [23]. In that work, the influence of the Leidenfrost temperature and film boiling heat flux were studied. The present paper uses the results of a comprehensive study to compare the relative influence of four boiling parameters (T_{leid} , Q_{film} , T_{CHF} , Q_{CHF}) on three issues responsible for the diminution of the recovery rate (hot tearing, bleed-out, butt curl).

2. SENSITIVITY STUDY

2.1 Boiling Parameters

A generic boiling curve is shown in Figure 2 including the four boiling regimes identified by Nukiyama for pool boiling: convective cooling, nucleate boiling, transition boiling, and film boiling. These regimes also exist in jet impingement boiling, with the difference that the points on the cooled surface around the stagnation point of the impinging jet are subjected to different boiling curves [22]. The reader is referred to Wolf and al. [24] for a review on jet impingement boiling. Five characteristic boiling parameters are also marked in Figure 2. The nucleation of the first bubbles occurs in the less restrictive cavities at a temperature called onset of nucleate boiling (T_{onb}) (1). Beyond this point, the heat flux increases to an extremum called critical heat flux (Q_{CHF}) (2). Above the temperature of the critical heat flux (T_{CHF}) (3), vapor covers a part of the surface reducing the heat transfer coefficient due to its low thermal conductivity compared to liquid water. The temperature for which a complete vapor film exists on the surface is called the Leidenfrost temperature (T_{leid}) (4). Above this temperature, heat transfer is mainly due to radiation and conduction. The low thermal conductivity of the vapor film and the low emissivity of the newly formed aluminum surface diminish the role of conduction and radiation through the vapor film. The film boiling heat flux (Q_{film}) (5) during aluminum DC casting has thus been considered to stay constant and equal to the heat flux at the onset of a complete vapor film. Due to the high temperature of the solidified surface in aluminum DC casting, only the last four boiling parameters have been considered in the sensitivity study.

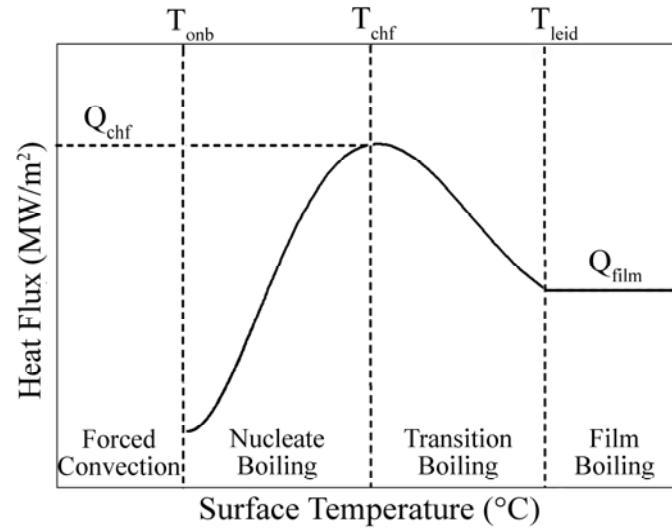


Figure 2 Generic boiling curve indicating the heat transfer regimes and characteristic boiling parameters

2.2 Methodology

The aim of the present study is to run a preliminary series of simulations in order to determine the tendency of the influence of boiling parameters on selected key process parameters. A key process parameter is defined as a measurable variable in the process that has an impact on the recovery rate. The selection of the process parameters for the actual study is presented in subsection 2.4 through a revision of the main issues that influence the recovery rate. An uncoupled thermal finite element model with Abaqus v11.1 has been used and is presented in section 3.

The influence of the boiling parameters has been introduced through the boundary conditions in the secondary cooling zone. The correlation between boiling parameters and the selected process parameters was determined during post processing. Significantly strong correlations were identified for supporting further developments.

As mentioned previously, 80% of the total heat is extracted by secondary cooling which is further divided into two distinct zones: impingement (1) and free falling (2). Obviously, a modification of the water quality influences the boiling parameters within both zones. However, the boiling parameters in the actual sensitivity study have been varied only in the impingement zone. Since a high mesh density is required for convergence [25], the additional computation time to study the effect of the boiling parameters on the free falling zone was prohibitive.

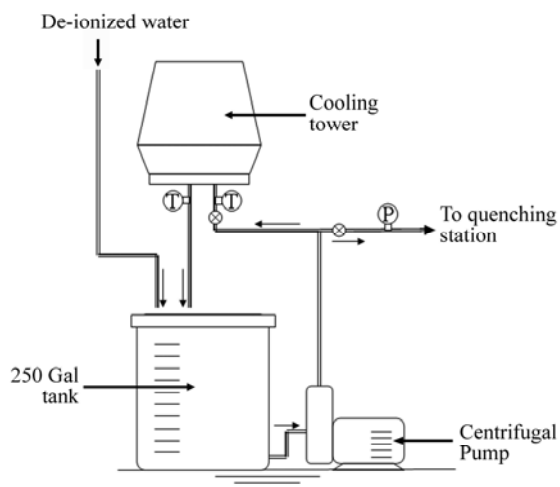
A reliable evaluation about the role of water on the process implies the computation of process parameters based on realistic variations of the boiling parameters. A series of measurements have been performed to determine the range of variability for each boiling parameter. The experimental results were implemented as boundary conditions in the mathematical model. Details of the experimental setup and the boiling curves used in the simulation are described in subsection 2.3.

2.3 Boiling curve measurement

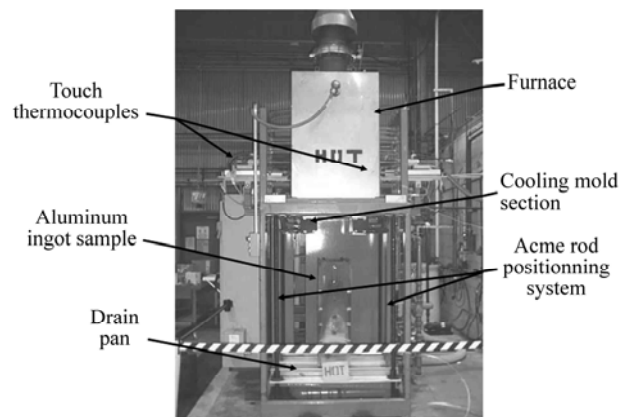
2.3.1- Experimental setup

The experimental setup used for the present study is the Mold Secondary Cooling Water Simulator at the Alcoa Technical Center. The device has been designed by Yu [18] and is one of the largest transient experimental setup which has been published in this field. It consists of a re-circulating water system (Figure 3a) and a quenching section (Figure 3b). The water system allows to produce a constant water quality for each quenching experiment. De-ionized water is used to eliminate the water chemistry effects, temperature and flow rate are also controlled before water is fed into the quenching station. The latter is made of a furnace, a real DC casting mold section and a large aluminum ingot of 0.305 x 0.305 x 0.67 meters. An automated system allows the ingot to be initially moved up inside the furnace where contact thermocouples motorized with compressed air are used to control the ingot temperature. When the sample reached a temperature of 500°C, it is moved down to the same level as the cooling mold section. A positioning system with acme rods allows a repeatable positioning of the water impingement zone on the ingot quench specimen. When the position of the preheated sample is confirmed, quench water from the mold section is finally directed onto the quench specimen. Imbedded thermocouples inside the sample connected to a data acquisition system are used to record temperature versus time data during the experiment.

An ingot sample used in the experiments is shown in Figure 3c. As-cast ingot surfaces have been used for the cooled surface. Temperature history has been recorded at the impingement point and two other locations situated at 15.24 cm and 30.48 cm below the impingement point. A cluster of 6 thermocouples was implanted at each location to record the temperature history below the cooling surface at a frequency of about 100 Hz. Positions of the thermocouples relative to the cooling surface were the same at each location and are shown in Figure 3d. An inverse heat transfer software package [26] has been used to calculate the heat flux as a function of surface temperature at the impingement point and downstream locations. The software solves for the heat fluxes at each time step to minimize the least square error with an added regularization term.



a



b

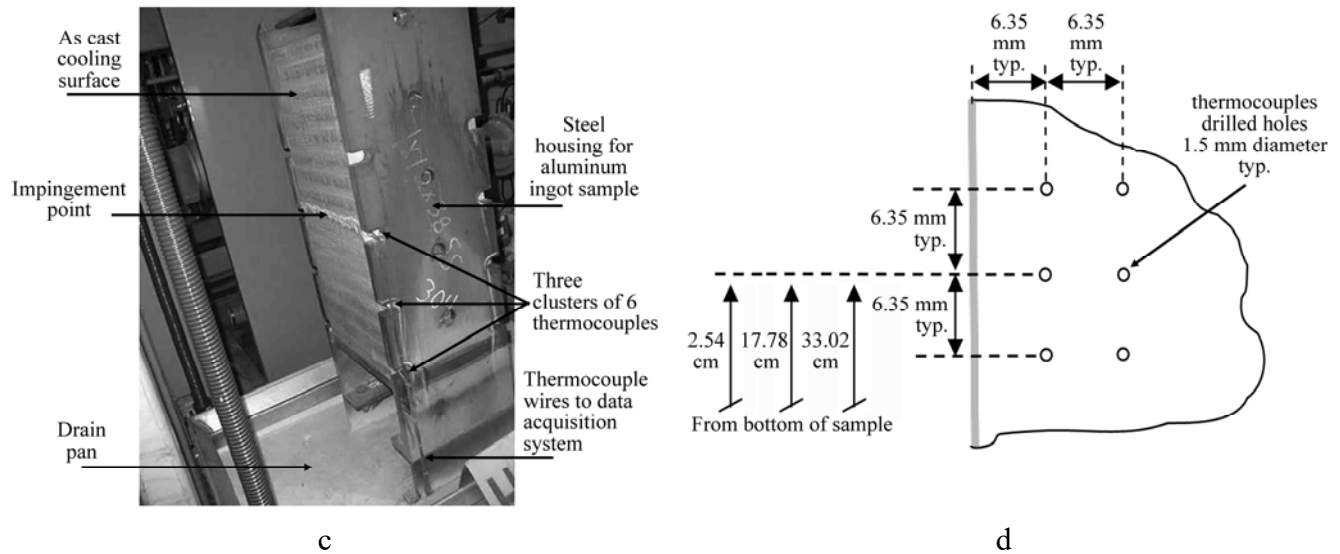


Figure 3 Experimental setup : Re-circulating water system (a) ; quenching section (b) ; ingot quench specimen (c) ; positions of the thermocouples relative to the cooling surface (d) [18]

2.3.2- Analysis of measured data

In order to establish the range of variation for each boiling parameter, only water temperature (27 °C to 32 °C) and linear flow rate (1.25 to 1.75 L/sec·m) variations have been applied. The goal was to use straightforward parameters as water temperature and water flow rate to determine what of the boiling parameters have a significant influence on the process. From the measurement of the boiling curve, Table 1 presents the minimal and maximal values at the impingement zone that have been used later in the sensitivity study. Standard deviations for each measured boiling parameter are also presented.

The standard deviations were obtained by running 5 consecutive tests on the same sample at a linear flow rate of 1.75 L/sec·m and a water temperature of 32 °C. The main factor influencing the repeatability was the surface oxidation. Results presented for the actual study (figure 4) have been measured on the same sample, the procedure was to achieve a repeatability verification based on 5 experiments followed by the sensibility study on water flow rate and temperature. The last test achieved on the sample after the sensibility study was at the same experimental conditions that the initial repeatability verification. This test allow to confirm that boiling parameters was still inside a confident interval despite surface oxidation.

Beck [27] divided the total error related to inverse heat conduction problem (IHCP) into two components: bias (error in the estimation) and the variance of the answer due to measurement errors. The standard deviations presented in Table 1 only refer to the total variance of the derived quantity (surface temperature and surface heat flux). The latter is function of the experimental parameters variation such as surface oxidation and additional variation related to IHCP. The bias and variance related to IHCP vary within the time step (Δt), thermocouple position ($x=E$), thermal diffusivity (α) and number of future time steps used inside IHCP. As presented by Beck [27], the dimensionless Fourier number ($Fo^+ = (\alpha \cdot \Delta t) / E^2$) is an efficient tool to minimize the total error (bias and variance) by optimization of the previous parameters. The Fourier number is the ratio of the heat conduction rate to the heat storage rate and can be used to analyze the time variation of the temperature measured by the thermocouples.

Comparison of the standard deviations of surface temperatures obtained by IHCP (presented in Table 1) to the standard deviation of the measured temperature in the ingot sample showed no significant additional fluctuation added by the numerical method. This observation is explained by two factors : the measured temperature inserted inside the inverse numerical method didn't contain significant fluctuations related to measurement errors (1); the high value of the Fourier number ($Fo^+=0.4$) which means that the lag of heat extraction at an interior location of the thermocouples with respect to the surface is relatively small consequently not affecting the sensibility of IHCP to measurement fluctuations (2).

Concerning the precision of IHCP to rapid heat flux fluctuation at the surface, the maximal bias of the numerical method can also be calculated. The exact solution of a plate heated at $x=0$ and insulated at $x=L_w$ can be used to get the errorless temperature values at the sensor position. Insertion of this temperature history in the inverse heat transfer computation should then give the exact heat flux variation that was first introduced in the exact solution. The maximal relative error between the initial heat flux history at the surface and the result obtained from IHCP thus represents the deterministic bias. Calculation showed that the maximum possible deterministic bias for a step fluctuation of the heat flux at the surface due to IHCP used in the actual study was 10%.

<i>Boiling Parameters</i>	<i>Minimum Value</i>	<i>Maximum Value</i>	<i>Standard deviation (%)</i>
Q_{film}	1.8 MW/m ²	2.2 MW/m ²	7
Q_{CHF}	2.8 MW/m ²	3.9 MW/m ²	7
T_{CHF}	210°C	260°C	5
T_{leid}	320°C	390°C	3

Table 1 Range of variation of the measured boundary conditions used during the sensitivity study.

Figure 4a shows the boiling curves measured in the experiment as function of water temperature and flow rate. The maximum and minimum values for each boiling parameter are also indicated. In order to test the impact of each boiling parameter within their range of variability, 64 hypothetic boiling curves were generated from the experimental results. These boiling curves are divided in four groups according to the values of Q_{CHF} and T_{CHF} . For each of the four reference boiling curves presented in figure 4b, Q_{film} was maintained constant just to the point $T=T_{\text{leid}}$. At this point, a jump of the heat flux up to the nucleate boiling value was assumed. An example showing the displacement of the jump of the heat flux used to simulate the variation of T_{leid} is shown in Figure 4c. The curves were slightly shifted in transition boiling regime for easier distinction. Although this type of curve was not measured directly, such a hypothetic curve can serve to judge the influence of the variation of T_{leid} and Q_{film} . After checking the duration of the transition regime, we found it is in the order of few tens of seconds. The shape of the boiling curve during this short time period cannot influence a zone deeper than few centimeters in the ingot. The actual shape of the monotonically increasing boiling curve has thus a localized effect on the overall temperature distribution in the ingot.

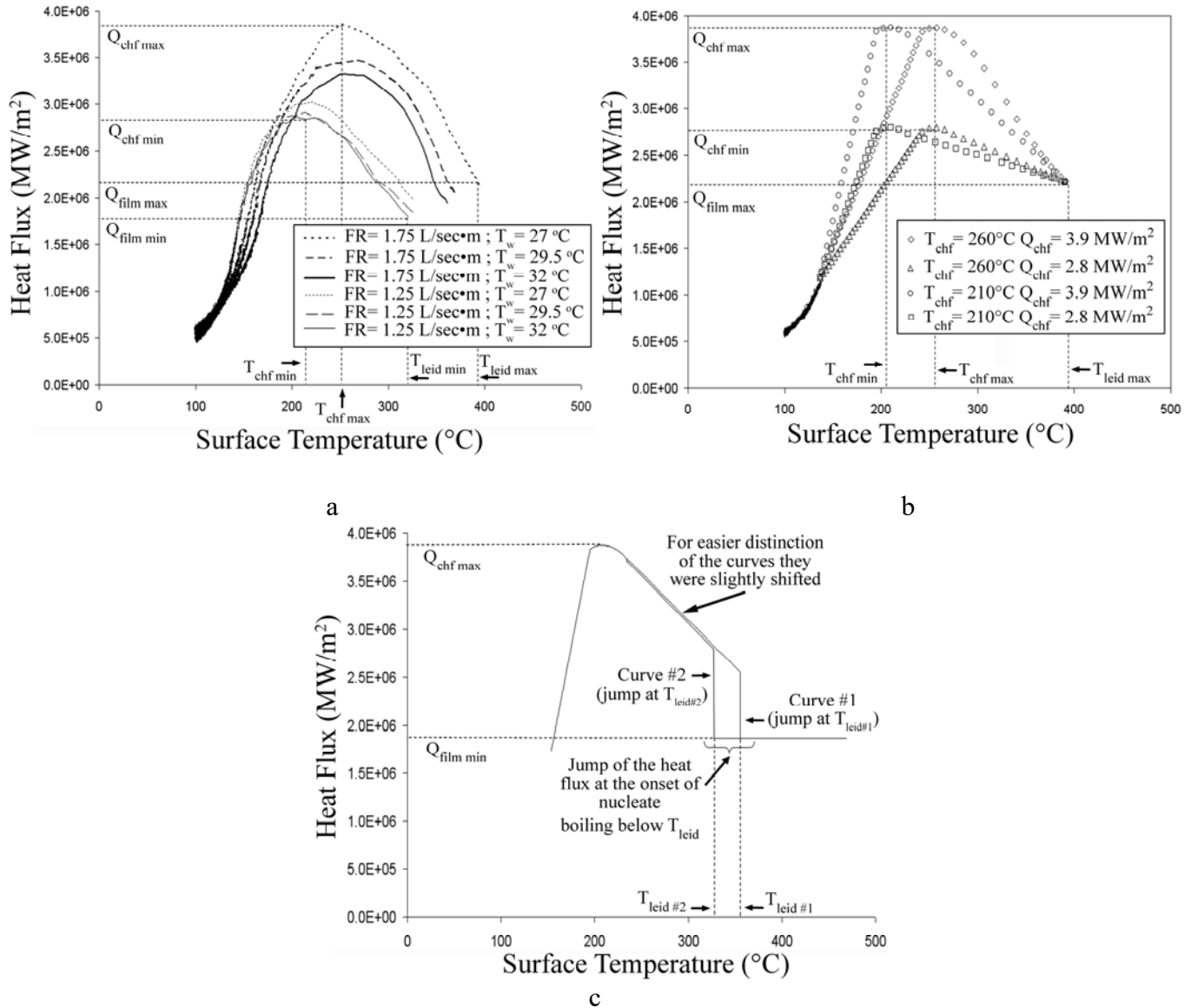


Figure 4 Measured boiling curves (a) reference boiling curves generated from the experimental results (b) example of the heat flux jump up to the nucleate boiling value used to simulate the variation of T_{leid} (c)

2.4 Selection of output parameters

The main problems responsible for reducing the recovery rate in DC casting are hot tearing, butt curl, bleed-out and surface quality. The reader is referred to Eskin [1] for an excellent review on most of these issues. From this list, the first three phenomena have been selected for the sensitivity study as described below.

2.4.1 Hot tearing

The emergence of numerical simulation in the 1970s resulted in the construction of finite element models for the study of hot tearing. Most of the publications have proposed criteria for the formation of cracks [28-30] rather than understanding the mechanisms [31] for the formation and propagation of a crack.

Depending on the type of simulation that was used (thermal, thermomechanical, fluid flow), different criteria for hot tearing have been proposed.

Uncoupled thermal models are the simplest that can be used to predict hot cracking. In this case, the criterion needs to rely on temperature variation in time. In 1972, Bryson [32] proposed the difference between the surface and center cooling rates as criterion. Clyne and Davies [28] were the first to propose a hot cracking index (HCS) that was based on the ratio of time spent in the temperature range where the risk of hot tearing is important. Jensen and Schneider [33] later found that the liquid pool goes through a maximum depth before it reduces to a steady state value. With increasing sump depth (Figure 1b), the mushy zone depth increases that causes a more difficult feeding during solidification.

Since tensile stress is responsible for hot cracking, most publications used coupled thermal-stress analysis for which many hot cracking criteria have been published: stress-based [34, 35], strain-based [36] and strain rate-based criteria. [37]. Although the previous criteria give good insights, pressure drop due to shrinkage and deformation are key parameters for hot tearing [38]. The RDG criterion from the name of the three co-authors of the original paper [30] is a well-known one that requires the difference between the metallostatic pressure and the pressure drop over the mushy zone (due to solidification shrinkage and deformed-induced fluid flow). If the pressure in the mushy zone locally drops below a critical value, a void may form and hot tear might occur.

In the present work, the sump depth [33, 39] has been used as hot cracking criterion for the sensitivity study. As explained, an increase of the sump depth promotes the risk for lack of metal feeding during solidification and increases the thermal gradient inside the ingot which results in higher stress during solidification shrinkage.

The aim of the present study is to determine the tendencies of the influence of boiling parameters on the risk of hot tearing. Even if more complex models accounting for fluid flow during solidification and thermo mechanical stresses allow a more detailed description of the occurrence of hot tearing, the present study concentrates on the dominant thermal mechanisms. The large number of simulations that clarify the sensitivity of the sump depth to the water boiling curve give insight on the impact of the most important boiling parameters on the process.

2.4.2 Bleed-out

Bleed-out is a leakage of molten metal that occurs when the solidified shell (Figure 1b) is not sufficiently rigid to withstand the hydrostatic pressure created by the liquid pool. The situation might cause a severe explosion when water is trapped by molten metal. The water then transforms to the vapor phase and undergoes significant volumetric expansion (about 1000 times) throwing metal violently out of its way.

Four principal situations can be related to the occurrence of bleed-out: high value of the upstream conduction distance (UCD), hang-up, excessive butt curl during the start-up phase and insufficient cooling. Among the causes for bleed-out, a variation of the water quality may cause a diminution of the cooling rate at the surface of the ingot. This results in a diminution of the shell thickness, which might break due to the metallostatic pressure of the liquid pool. In the present work, the shell thickness at the impingement zone will be used as bleed-out criteria. The goal is to evaluate the sensitivity of bleed-out to the secondary cooling conditions instead of an accurate computation of the occurrence of bleed-out. According to the

author's knowledge, no published paper compared the influence of boiling parameters in the impingement zone on the occurrence of bleed-out.

2.4.3 Butt curl

Butt curl corresponds to the situation when the bottom of the ingot lifts off from the bottom block at casting start (Figure 1b). An excessive butt curl can cause different casting issues : false start, explosion caused by meniscus detachment from the mold followed by water entrapment after liquid metal run over, [2]; collapse of the shell supporting the butt due to weight of the ingot causing butt crack or a continuous crack over the rolling face [40].

The basics of butt curl formation are that the exterior of the ingot is cooled down by water while the interior is cooled down slowly by conduction, causing different contraction rates. [6] This differential in contraction produces stresses, as one part of the casting restrains another. [41] An overview of the different steps and phenomena at casting start allow to better understand the butt curl occurrence and helps choosing of a criterion to characterize butt curl sensitivity to boiling parameters.

At casting startup, there is a vapor film which completely covers the rolling face (Figure 5a), the boiling regime at the surface is mainly film boiling that creates a lower heat flow rate (Figure 2). The difference in the cooling rates between the center of the ingot and the surface is therefore less important. When the vapor film disappears in the center of the impingement zone (Figure 5b), the heat flux at the surface increases significantly compared to center of the ingot. Grealy [40] mentioned that there is a drastic change of cooling when the early film boiling breaks down and much more severe cooling by nucleate boiling takes over. It has also been reported in the literature that the moment when the thermal gradient increases at the middle of the impingement zone (point B in Figure 1b) coincides with the increase of the mechanical stresses inside the ingot. [42]

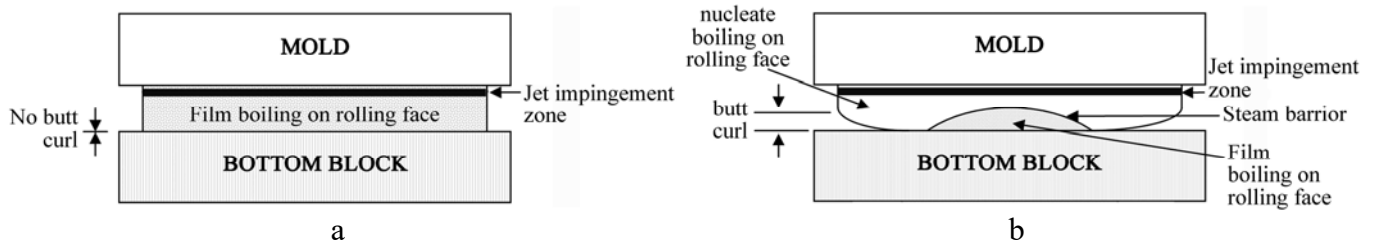


Figure 5 Growing of butt curl at casting start before (a) and after (b) the vapor film disappears in the center of the impingement zone on the rolling face after Grealy [40]

The complete distribution of the mechanical stress at casting startup resulting from the variation of the contraction rate inside the ingot is well presented in the literature [41-43]. In a simplified manner, when the vapor film disappears in the center of the impingement zone, the rapidly shrinking surface is in compression while the solidifying boundary along the mushy zone near the center of the ingot is subject to a slower contraction rate and becomes tensioned as it undergoes the effect of rapid contraction at the surface of the ingot. Based on the results presented by Boender [41], a qualitative representation of the stresses created on the surface of the ingot is shown in Figure 6. These constraints create a bending moment responsible for the deformation of the ingot base. The development of a moment sufficient to deform the ingot base begins until reaching the maximum deformation rate at about 0.3 m withdrawal

length [43]. The growth rate then starts to decrease down to a zero value at approximately 1 m withdrawal length.

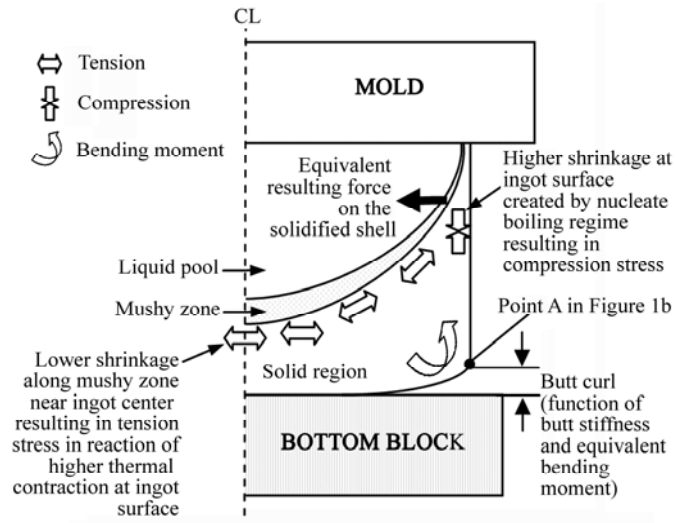


Figure 6 Butt curl grow mechanism and direction of principal stress at casting startup after W. Boender et al [41]

The two main factors influencing the amplitude of the butt curl are the casting length at which the vapor film disappears, varying the bending moment applied to the ingot base [43] and the ingot butt stiffness when the vapor film at the impingement zone disappears. Although intuition could lead to consider that a higher tensile stress at the ingot base after elimination of the vapor film automatically increases the butt curl, this is not the case. Sengupta [44] compared the variation of the butt curl with different cooling rates of the bottom block. In the study, it was demonstrated that the stiffness of the ingot base achieved by decreasing its temperature before reaching the maximum tensile stress along the sump profile limits the ingot base deformation. A similar study on the impact of the bottom block cooling by Wiskel [42] also demonstrated that the stiffness of the ingot base has a stronger influence than the absolute value of the tension stress itself along the sump depth. Ishikawa also mentioned that it is fully understood that the higher temperature of solidified is kept, the easier butt curl grow. [43]

Furthermore, one of the well-known ordinary skills in the casting art today is that ingot butt can be controlled by decreasing the ingot surface cooling at start-up. [45] The formation of a vapor film at start-up is one of the strategies used in order to reduce the ingot butt temperature at low cooling rate before the bending moment caused by tension forces along the sump profile, becomes sufficient to deform the ingot base. Cooling by a lower heat flux makes it possible to create a more rigid ingot butt before increasing the bending moment represented in Figure 6. Many existing technologies do this by CO₂ injection by Alcoa, [46] Turbo process by Wagstaff [47] and Alcan's pulsed water technique [48].

The previous literature review shows that an higher bending moment when the vapor film disappears at the ingot surface does not necessarily means an increase of the butt curl. However, a lower ingot base temperature when the thermal gradient at the surface increases (ie the vapor film disappears) implies a greater stiffness of the ingot butt and a smaller final butt curl [42-44]. The variation of the mechanical properties as a function of the temperature explains this behavior. These are presented by Lalpoor [49] for

7xxx alloys. A decrease in temperature between 400 °C and 200 °C causes an increase in the Young modulus of about 15% and an increase in yield strength from 50 MPa to 150 MPa.

The objective of the actual study is to demonstrate which boiling parameters influence the butt curl. The dependence of butt curl on the ingot base temperature when the vapor film disappears has been demonstrated in several studies [40, 42-44], which supports the use of this parameter in the sensitivity study. The temperature of the ingot base when the vapor film disappears at a casting length of 0.3 m was also considered in the literature [43], since it is the typical moment when the rate of growth of the butt curl is maximal. The temperature along the vertical axis of the rolling face (Figure 11c) has been used for both heights (ingot base and cast length of 0.3 m). The ingot base temperature has been computed on the bottom edge of the rolling face, which is called ingot lip.

The results of the present study could be used into a future thermo-mechanical study that will then allow to quantify the butt curl resulting from the variation of the targeted boiling parameters. However, this is not in the scope of the actual study.

3. MATHEMATICAL MODELING

3.1 Existing models

Weckman and Nielsen [50] gave a review on thermal models for DC casting from 1947 to 1982. The reader is also referred to Sengupta's thesis [4] for an excellent review on uncoupled and coupled models for DC casting from the beginning of 1980s to the early 2000s. Based on Sengupta, most models created after beginning of the 1990s included bottom block heat transfer. The majority of these models also used the freezing method for measuring of the boundary conditions in the secondary cooling zone as function of surface temperature and flow rate. Finally, Grandfield [2], presented a more recent review on DC casting modeling.

3.2 Model using Abaqus

As mentioned earlier, an uncoupled heat conduction model has been developed. Uncoupled heat transfer analysis was used in Abaqus to model heat conduction with temperature-dependent thermophysical properties. Non-linear temperature dependent convection boundary conditions described in subsection 3.4 have also be used. Two phenomena are not represented by an uncoupled thermal model: convection inside the sump and the mechanical stress and deformation of the ingot caused by variation of the contraction rate during solidification. The utilization of an uncoupled model is explained by the choice of the previously presented output parameters (sump depth, shield thickness and ingot base temperature). Since the latter are mainly influenced by thermal phenomena, the temperature distribution as function of time obtained from the uncoupled thermal model was not used as boundary condition in a second mechanical model. To consider convection inside the liquid pool, a method used in the literature is to use an increased, apparent conductivity of the liquid metal (for $T > T_{liq}$). Drezet [51] has used this approach to converge the computed value of the sump depth in steady state to the measured value. The validation of the present model as described in subsection 3.6 already shows quite satisfactory agreement with other published results even if convection in the sump was not considered.

The implicit discretization available in Abaqus/Standard has been used because it is unconditionally stable. Abaqus includes an iterative resolution method called FETI for models larger than one million degrees of

freedom. The latter does the decomposition of the equation system into several sub-systems by using Lagrange multipliers to ensure continuity between domains. The actual model has approximately 500 thousand degrees of freedom so a direct resolution method with the inversion of the stiffness matrix has been used.

The thermophysical properties of the alloy A7055 used for the simulation are shown in Table 2. The thermal conductivity, density and specific heat are functions of temperature. The latent heat has also been considered within the solidification range ($T_{\text{liquidus}} = 635 \text{ }^{\circ}\text{C}$; $T_{\text{solidus}} = 468 \text{ }^{\circ}\text{C}$). The latter is included in the equivalent specific heat using the enthalpy method. The evolution of the solid fraction and thermophysical properties during the solidification interval were followed by a proprietary code. The results were similar to Lalpoor and al. [52] obtained with JMat-Pro. Newton's method, solving the Jacobian at each step of iteration, was used for the resolution of the non-linear model.

<i>Temperature</i> ($^{\circ}\text{C}$)	<i>Density</i> (kg/m^3)	<i>Thermal conductivity</i> ($\text{W}/\text{m}\cdot^{\circ}\text{C}$)	<i>Specific Heat</i> ($\text{J}/\text{kg}\cdot^{\circ}\text{C}$)
10	2805.0	166.5	820.0
100	2795.0	186.0	904.0
300	2760.0	194.0	1037.0
400	2725.0	196.0	1129.0
500	2690.0	181.9	1884.1
600	2626.0	156.0	4618.7
634	2480.0	85.0	1169.0
700	2452.0	85.0	1169.0

Latent heat of fusion (at $468 \text{ }^{\circ}\text{C}$) = $387 \cdot 10^3 \text{ J}/\text{kg}$

Table 2 Thermophysical properties of the alloy A7055 used for simulation

3.3 Geometry

The ingot and bottom block geometries used in the model are shown in Figure 7. The total cast length considered for the simulations is 0.7 m. The symmetry allows modeling only a quarter of the actual ingot size in order to reduce computation time. The window delimited by a dotted line is used to represent the area near impingement zone on the rolling face. The impingement zone moves upward at a casting speed of 57.15 mm/min. Shape and size of the zone covered by the vapor film near impingement zone inside the delimited window will be showed in section 4 to explain the results. The length and width of the ingot section in the model are respectively 0.762 m. and 0.2032 m. These dimensions are similar to those used in a typical cast house.

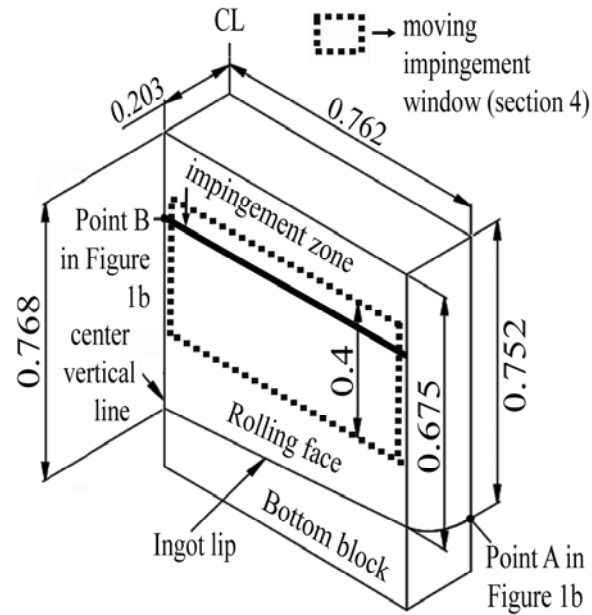
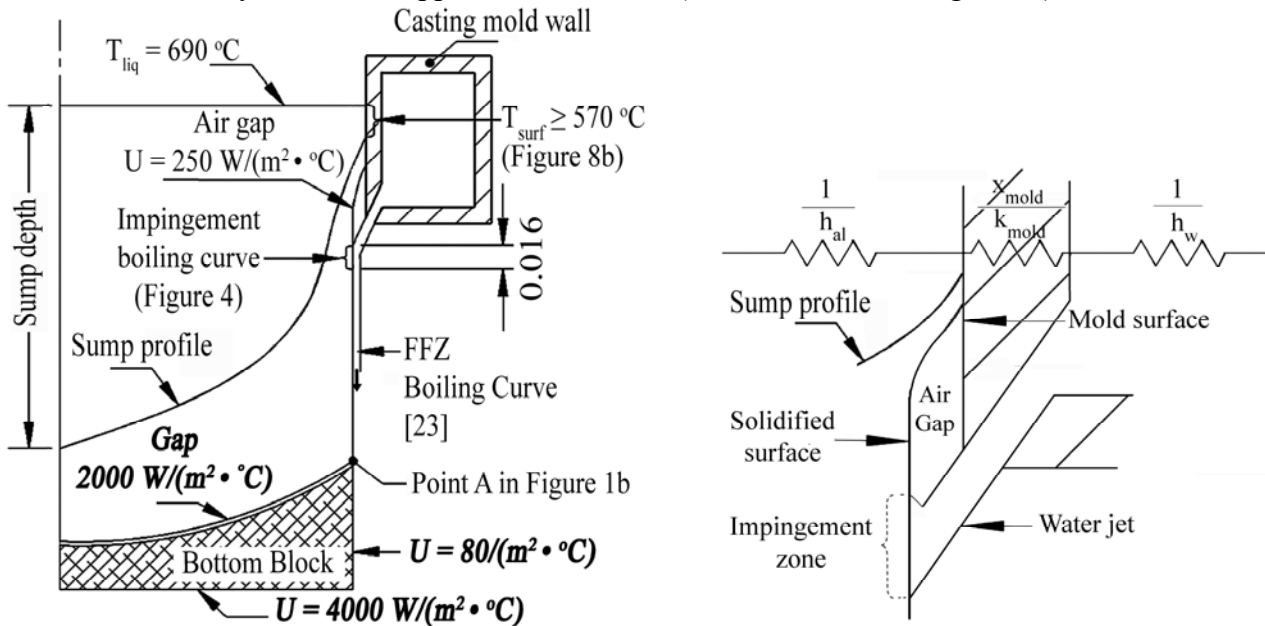


Figure 7 Isometric views representing the geometries of the ingot used in the computational model (dimensions are given in meters)

3.4 Initial and boundary conditions

The mesh is stationary so the boundary conditions have been moved at the ingot withdrawal rate. The supply of liquid aluminum is represented by the addition of element layers. The initial temperatures for the ingot and the bottom block are 690 °C and 30 °C respectively. A summary of the boundary conditions used in the simulation is presented in Figure 8. They are divided into two categories:

- boundary conditions that move at the ingot withdrawal rate;
- fixed boundary conditions applied on the nodes (bold characters in Figure 8a).



a b

Figure 8 Summary of boundary conditions used in the simulation (a) and illustration of the series of thermal resistances in the primary cooling zone (b). (dimensions are shown in meter)

3.5 Convergence

An extensive convergence study has been performed in order to determine the required mesh density. Three types of criteria have been studied as function of time: the temperature (1), the heat flux (2) and the output parameters established earlier for the sensitivity study (3). From the convergence study, the smallest required element size in the (x,y,z) directions are 5, 6.3 and 8 mm. The horizontal mesh density decreased exponentially in both x and y directions from the center of the ingot while each element has a constant height of 8 mm. The computation time for the selected mesh density was 55 hours in a parallel environment of 10 CPUs.

3.6 Model validation

The strategy to validate the thermal model used in this paper is a comparison with experimental results found in the literature and listed in Table 3. Equation 1 of the sump depth has also been used for the comparison.

Roth [53] and Dobatkin [54] showed that sump depth increases with the square of the diameter, linearly with the cast speed and is inversely proportional to the alloy thermal conductivity. Equation 1 described the more detailed estimation of the sump depth in steady state presented by authors:

$$H_{sump} = \frac{\left(\Delta H_f \rho_s + \frac{1}{2} C_s \rho_s (T_m - T_{surf}) \right) \cdot V_{cast} \cdot R^2}{4 \cdot k_s \cdot (T_m - T_{surf})} \quad (1)$$

where T_m is the melting temperature, T_{surf} is the temperature of the billet surface or the temperature of the cooling medium, R is the radius for cylindrical ingot (called billet) or the ingot thickness for rolling ingot, V_{cast} is the casting speed, k_s is the thermal conductivity of solid, ΔH_f is the latent heat of fusion, ρ_s is the density and C_s is the specific heat of the solid.

Equation 1 represents a calculation of the sump depth based on process parameters (V_{cast} , R , T_m , T_{surf}) and thermal properties (k_s , ΔH_f , ρ_s , C_s). Among these parameters, the more significant are V_{cast} , R and k_s since the others do not vary significantly for different aluminum alloys. Equation 1 can thus be simplified to

$A \cdot \frac{V_{cast} \cdot R^2}{k_s}$ where A is a constant used to represent the influence of thermal properties and casting

temperatures in Equation 1. This simplified form of Equation 1 is interesting since empirical values of A can be calculated from measured sump depth values.

Table 3 compares the measured values of the sump depth by two authors, together with the identification of the measurement techniques. The principle of the "freezing method" is to insert thermocouples inside the ingot near its surface, which are then trapped in the solidifying metal and move downward with the

ingot at the withdrawal rate. The rod technique consists of touching the solidification front (T_{solidus} in Figure 1b) inside the sump depth with a rod.

The empirical value of parameter A has been calculated for the two studies presented in Table 3. As expected, the values are very similar among the two studies. The average value of A is 0.0081 with a standard deviation of 0.0005 (6%). As mentioned, this similitude is related to the small variation of the thermal properties and casting temperature represented by A among the two studies.

Since the thermal properties and casting temperatures used in the actual study are also very similar to the studies presented in Table 3, the previous average value of A has been used in Equation 1 to obtain an estimation of the expected values of the sump depth. Table 4 compares the sump depth obtained in steady state from the actual mathematical model with the calculated values of the sump depth based on the empirical value of A from literature. The values are within a 2.4 % range of variation, which was judged acceptable.

References	Alloys	Thermal conductivity (W/m·K)	Casting speed (mm/min)	Ingot thickness or billet radius (m)	Sump depth measurement technique	Measured sump depth in steady state (mm)	Calculated value of A
Drezet [55]	1xxx	237	50	0.510	Frozen thermocouple	425	0.0078
Grandfield [39]	6061	180	90	0.114	steel rod	55	0.0084

Table 3 Literature review of measured sump depths for model validation

Thermal conductivity of solid (W/m·K)	Casting speed (mm/min)	Ingot thickness (m)	Sump depth in steady state obtained with actual model (m)	Value of sump depth based on calculated value of A (m)
182	57.15	0.406	0.430	0.420

Table 4 Comparison of sump depth obtained with the actual mathematical model and those based on the average value of A from literature.

4. RESULTS AND DISCUSSION

4.1 Sump depth

It is well known that the sump at start-up grows first to a maximum depth before falling and stabilizing at a steady state value [1, 33, 39]. The height of the mushy zone also increases with the sump depth that increases the risk of hot cracking. For this reason, the maximum sump depth reached at start-up was used for the sensitivity study in Figure 9.

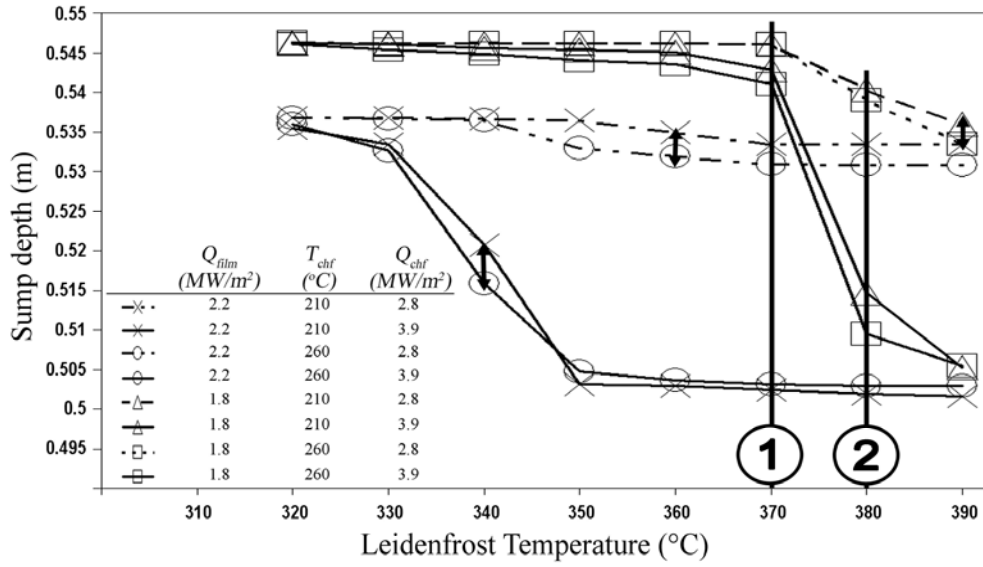
The small variation of the sump depth as function of T_{CHF} is first shown in Figure 9a. Small arrows highlight that the variation of the sump depth is negligible when only T_{CHF} is changed for the same combination of T_{leid} , Q_{CHF} and Q_{film} . The value of T_{CHF} therefore has no influence on the risk of hot cracking and should not be considered during the study of the influence of water quality.

Figure 9b shows the impact of Q_{CHF} on the sump depth. At low values of Q_{CHF} (2.8 MW/m^2), the sump depth is high for all cases, regardless T_{leid} and Q_{film} . The term "dominant factor" is introduced here to define the situation where a boiling parameter has such a strong influence on a process parameter that the effect of the others is negligible. Here Q_{CHF} has been called the dominant factor of the sump depth since it is able to control alone its value. The explanation of the role of Q_{CHF} is possible through the study of boiling regimes that occur on the rolling face. For every case at low Q_{CHF} (2.8 MW/m^2) in Figure 9b, a vapor film still exists on the rolling face at the time corresponding to the maximal sump depth.

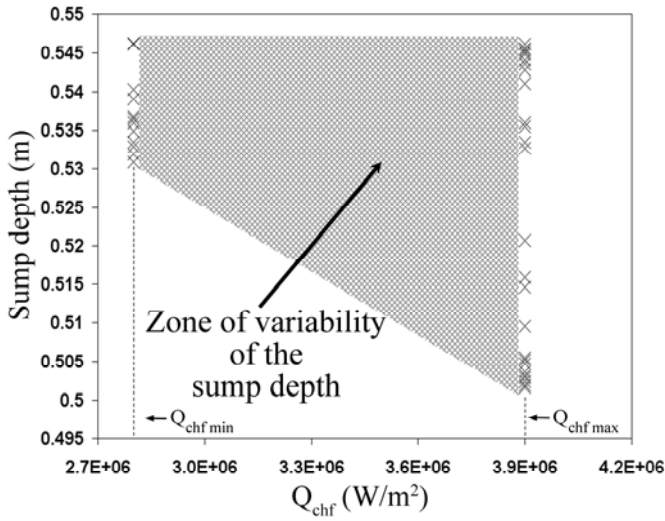
The importance of the vapor film at the center of the rolling face is confirmed by analyzing cases where the value of Q_{CHF} is high (3.9 MW/m^2). At this value of Q_{CHF} , Figure 9a shows that the sump depth varies greatly within an interval of T_{leid} that is function of Q_{film} . The case of $Q_{\text{film}}=1.8 \text{ MW/m}^2$ for which this situation arrives between $370 \text{ }^\circ\text{C}$ (identified as 1) and $380 \text{ }^\circ\text{C}$ (identified as 2) is used as an example. The higher heat transfer conditions at start-up obtained by increasing T_{leid} within this interval allow eliminating the vapor film on the rolling face before the maximal sump depth at start-up reached. The variation of the area covered by the vapor film within this interval is shown in Figure 9c where the area delimited by dotted line refers to moving impingement window on rolling face shown in Figure 7. This elimination of the vapor film on the rolling face at start-up causes a large decrease of the sump depth. Although not shown, the same phenomenon occurs at $Q_{\text{film}} = 2.2 \text{ MW/m}^2$ for an increase of T_{leid} from $330 \text{ }^\circ\text{C}$ to $350 \text{ }^\circ\text{C}$.

The conditions of heat transfer near the impingement zone can thus significantly decrease the sump depth only when the vapor film is completely eliminated during the growing period of the sump depth at start-up. This is only possible at high Q_{CHF} , where on the other hand, the interaction between Q_{film} and T_{leid} is very important.

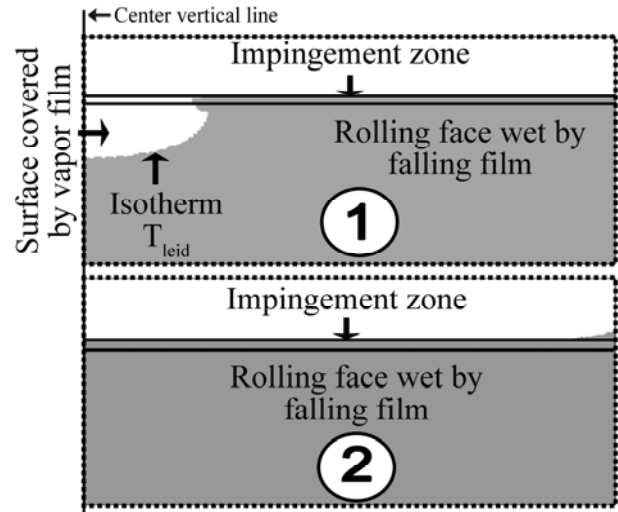
The strong interaction between $T_{\text{leid}}-Q_{\text{film}}-Q_{\text{CHF}}$ demonstrates that the potential variation of these boiling parameters following a change in water quality can influence the sump depth and thus the risk of hot cracking.



a



b

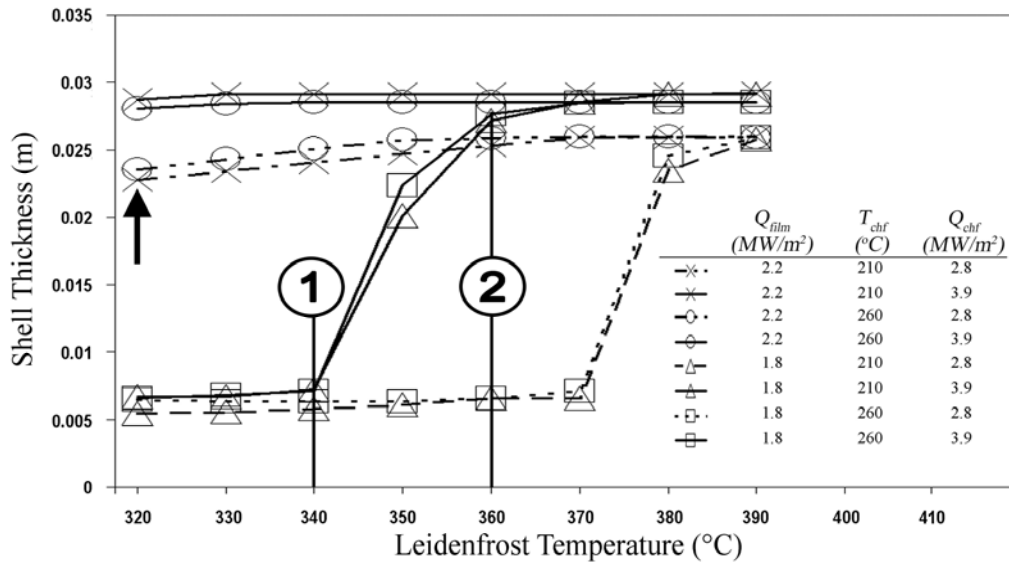


c

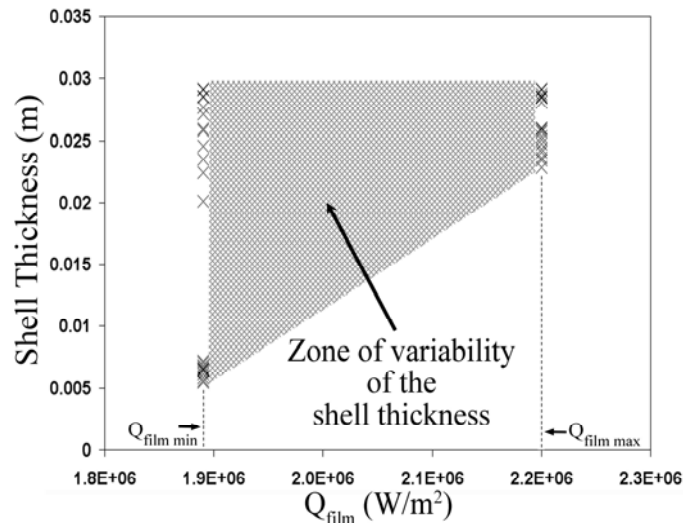
Figure 9 Graphics with markers representing the variation of the maximum sump depth reached at start-up as function of the boiling parameters T_{leid} (a) and Q_{chf} (b). Elimination of the vapor film on the rolling face before the time corresponding to the maximal sump depth. (c) Area delimited by dotted line refers to moving impingement window on rolling face as shown in Figure 7.

4.2 Shell thickness

Figure 10 shows the shell thickness in the impingement zone, at the center of the rolling face. This position is critical since it corresponds to the smallest value of the shell thickness (farthest point from the regions with the highest cooling rate at the ingot corners). The values of the shell thickness shown in Figure 10 have been obtained at the time when the sump depth reaches a maximal value. The idea is that increasing the shell thickness before reaching the maximum sump depth reduces the risk of bleed-out. An easy conclusion can be drawn first on T_{chf} . As explained for the sump depth, the analysis of the graph in Figure 10a still supports the conclusion that T_{chf} has no significant influence on the shell thickness and thus on the occurrence of bleed-out.



a



b

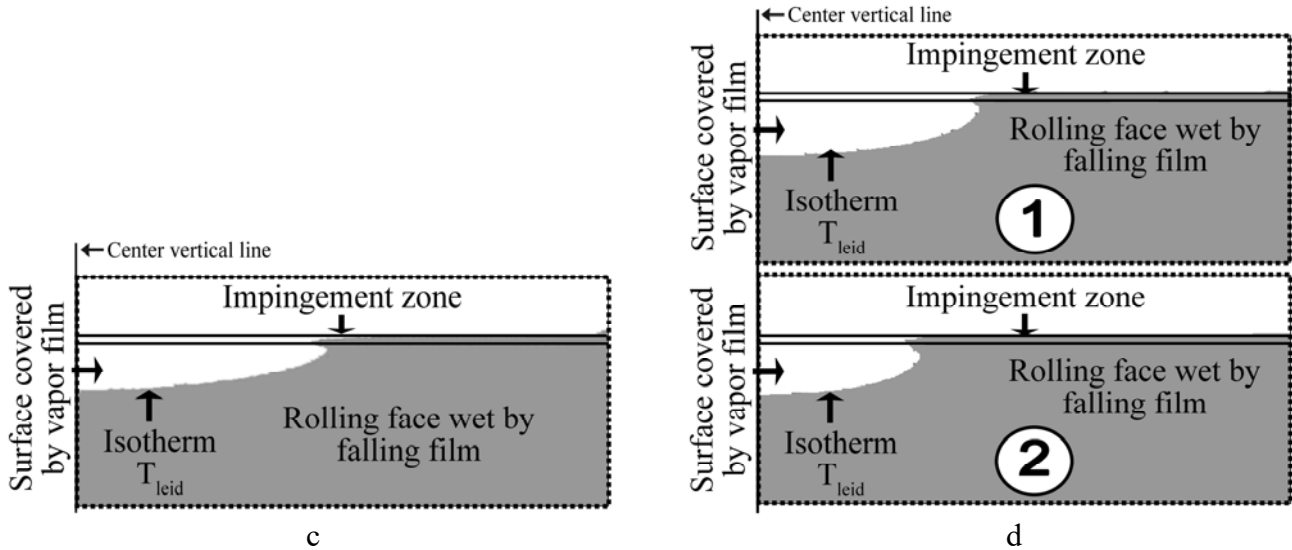


Figure 10 Variation of the shell thickness at the time corresponding to the maximal sump depth at start-up as function of T_{leid} (a) and Q_{film} (b). Shape and size of the zone covered by the vapor film on the rolling face at the time when the sump depth reaches a maximal value at start-up is shown in (b) and (d). Area delimited by dotted line refers to moving impingement window on rolling face shown in Figure 7.

Figure 10b shows that the shell thickness is about 2.5 to 3 cm regardless of the value of the other boiling parameters at $Q_{film} = 2.2 \text{ MW/m}^2$. Q_{film} is thus the dominant factor for the shell thickness, as defined previously. The minimum heat transfer conditions at $Q_{film} = 2.2 \text{ MW/m}^2$ ($Q_{CHF} = 2.8 \text{ MW/m}^2$; $T_{leid} = 320 \text{ }^\circ\text{C}$; $T_{CHF} = 210 \text{ }^\circ\text{C}$) allow to understand the influence of Q_{film} on the shell thickness. This case is identified by the up arrow at the left of the Figure 10a. For these boiling parameter values, a vapor film still exists at the center of the rolling face at the time corresponding to the maximal sump depth during start-up (Figure 10c). The area delimited by dotted line still refers to moving impingement window on rolling face shown in Figure 7 This observation demonstrates that $Q_{film} = 2.2 \text{ MW/m}^2$ is sufficient to allow a high thickness of the solidified wall in the impingement zone regardless of the existence of a vapor film on the rolling face.

Figure 10a shows that at $Q_{film} = 1.8 \text{ MW/m}^2$, the shell thickness is function of the interaction between T_{leid} and Q_{CHF} . When Q_{film} is not sufficient to produce a safe wall thickness, the position of the contour of the zone covered by the vapor film on the rolling face becomes important. The distance between the contour line and the center of the ingot is controlled by the interaction of T_{leid} and Q_{CHF} . Figure 10d shows that increasing T_{leid} from $340 \text{ }^\circ\text{C}$ (identified as 1) to $360 \text{ }^\circ\text{C}$ (identified as 2) at $Q_{CHF} = 3.9 \text{ MW/m}^2$ promotes the onset of nucleate boiling at the center of the ingot. The higher heat flux in the nucleate boiling region is then sufficiently close to the center of the rolling face to increase the shell thickness. The same phenomenon occurs at $Q_{CHF} = 2.8 \text{ MW/m}^2$ when increasing T_{leid} from $370 \text{ }^\circ\text{C}$ to $390 \text{ }^\circ\text{C}$.

From the results, the interaction between T_{leid} , Q_{film} and Q_{CHF} must be considered in order to evaluate the risk of metal leakage. This interaction demonstrates why the measurement of each of these three boiling parameters should be performed in order to study the influence of the water quality on the risk of bleed-out.

4.3 Ingot base temperature

The selected key output parameter related to butt curl (subsection 2.4.3) is the ingot base temperature (T_{base}) at the time corresponding to the increase of the cooling rate at 0.3 m withdrawal length. For the actual sensibility study, the ingot base (T_{base}) and the 0.3 m withdrawal length temperatures ($T_{0.3 \text{ m}}$) have been considered respectively at the center of ingot lip and along the center vertical of the rolling face (Figure 11c). Again, the role of T_{CHF} is discussed first. As demonstrated for the sump depth and shell thickness, T_{CHF} has no influence on the butt curl (Figure 11a). Therefore, we can conclude that the variation of T_{CHF} has no influence at all on the process and it is the only boiling parameter whose measurement is not relevant.

Figure 11b shows that Q_{CHF} acts as a dominant factor for butt curl, since the ingot base always remains at a safe low temperature when $Q_{\text{CHF}} = 2.8 \text{ MW/m}^2$. At this value of Q_{CHF} , the overall heat transfer rate near the impingement zone is sufficiently low to always allow a reduction of the base temperature down to $110 \text{ }^\circ\text{C}$ before the increase of the cooling rate at a 0.3 m withdrawal length.

Although the vapor film has no influence when Q_{CHF} is low, it is well known by plant operators that the butt curl can be reduced by promoting the formation of a vapor film on the rolling face at start-up (CO_2 injection by Alcoa or Alcan's pulsed water technique). These techniques are illustrated in Figure 11a at $Q_{\text{CHF}} = 3.9 \text{ MW/m}^2$. Consequently, the interaction between T_{leid} and Q_{film} is important. When Q_{film} is high (2.2 MW/m^2), T_{leid} must be as low as $330 \text{ }^\circ\text{C}$ in order to allow a reduction of the ingot base temperature down to $110 \text{ }^\circ\text{C}$. However, the same result at a lower Q_{film} (1.8 MW/m^2) occurs at $T_{\text{leid}} = 370 \text{ }^\circ\text{C}$. The latter case is illustrated in Figure 11c. The slower temperature drop in the impingement zone when $T_{\text{leid}} = 370 \text{ }^\circ\text{C}$ (identified as 1) gives an additional time to reduce the ingot base temperature compared to the case when $T_{\text{leid}} = 380 \text{ }^\circ\text{C}$. (identified as 2)

The vapor film position near the impingement zone on the rolling face is responsible for the interaction between Q_{film} and T_{leid} at high Q_{CHF} . If the heat flux produced by the vapor film is higher (greater Q_{film}) then T_{leid} should be decreased in order to extend the vapor film coverage on the rolling face toward the ingot corner. Therefore, the resulting lower overall heat extraction rate gives more time to reduce the ingot base temperature while small temperature gradients remain inside the ingot. The variation of the vapor film covered zone is however not illustrated.

Finally, the interaction between T_{leid} , Q_{film} and Q_{CHF} shows once again the importance of measuring each of them to assess the impact of a change in the water quality. The butt curl, as for the two previous process issues, varies as function of this interaction.

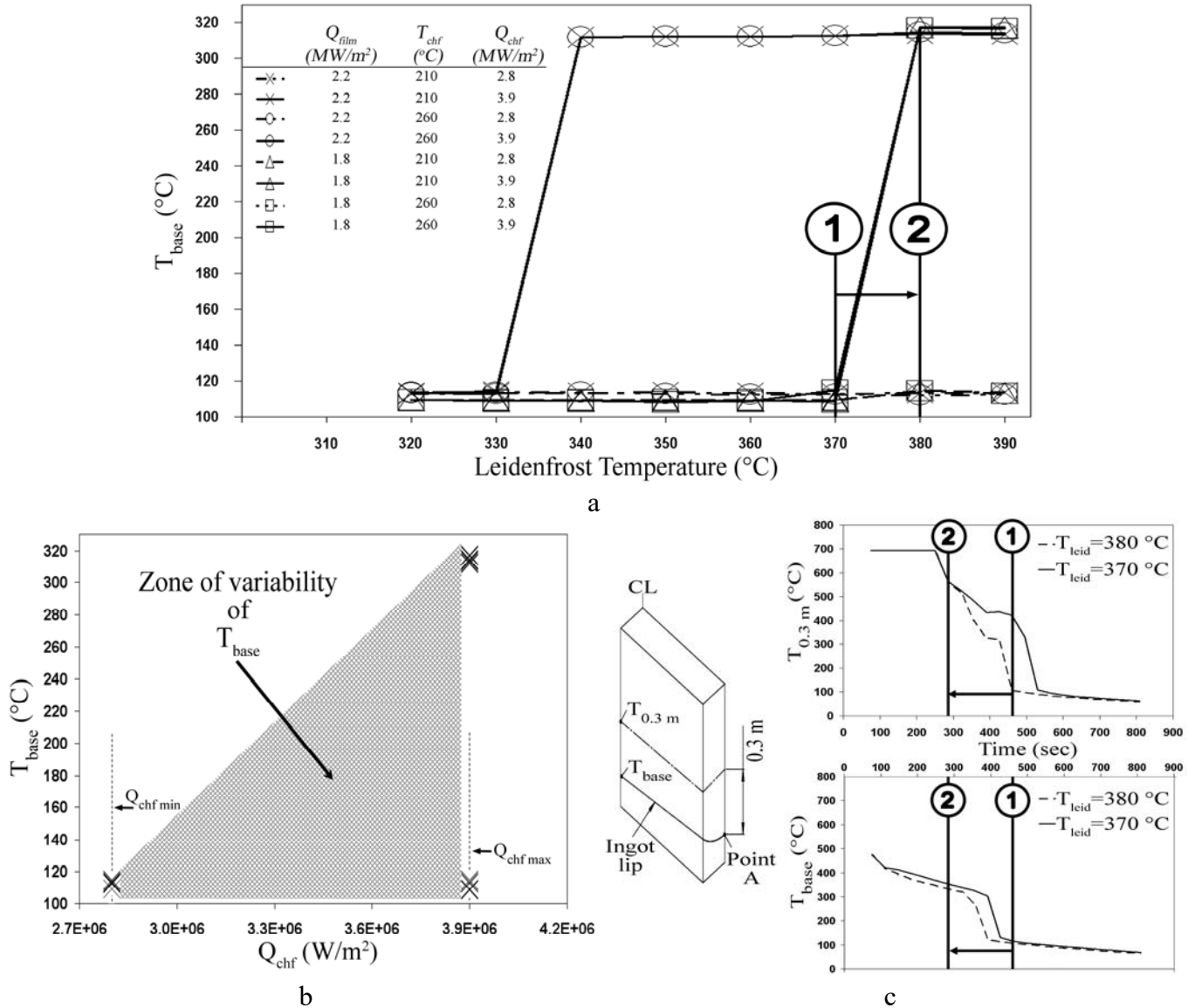


Figure 11 Variation of the ingot base temperature as function of T_{leid} (a) and Q_{chf} (b) at the time corresponding to the increase of the cooling rate at 0.3 m withdrawal length. Details of the procedure used to determine the ingot base temperature are illustrated in (c).

5. SUMMARY AND CONCLUSIONS

This work aimed at determining the role of the four principal boiling parameters which characterize the boiling curve (T_{CHF} , T_{LEID} , Q_{FILM} , Q_{CHF}) on the main problems which contribute to the decrease of the recovery rate in aluminum direct-chill casting. Many researchers have already measured the boiling curves that characterize the heat transfer during the process. However, none of these studies determined clearly the role of the individual boiling parameters and their interactions. Furthermore, very few studies mentioned the repeatability obtained on the measurement of these parameters. This paper can thus be seen as a first step in the direction of the development of a measurement method and apparatus that can supply reliable results for each targeted boiling parameters.

To determine the influence of the individual boiling parameters, a sensitivity analysis was performed by using an uncoupled finite element heat transfer model. The model was used to vary the boundary conditions, representing the role of the water and the effect of these variations on the recovery rate problems was analyzed. Each of the important issues of casting quality was represented by an output parameter during the simulation.

A new approach has been used in order to isolate the influence of the different boiling parameters. Four reference boiling curves, generated from measurement results according to the values of Q_{CHF} and T_{CHF} , were used as boundary condition and only the values of the studied boiling parameters were modified independently. Particular attention was paid to the use of realistic values for the experimental study of the parameters range.

The influence of the four boiling parameters on each of the recovery rate issues has been evaluated, one at a time. Within the studied range, the behavior of process parameters as function of the boiling parameters have shown that:

- No significant simple or combined effect involving the temperature of the critical heat flux T_{CHF} have been obtained for any of the tested conditions. This boiling parameter cannot be used to get insight into the occurrence of any of the studied recovery rate issues.
- The influence of a three-way interaction between the Leidenfrost temperature T_{LEID} , the film boiling heat flux Q_{FILM} and the critical heat flux Q_{CHF} on all the output parameters shows the importance to measure each of them in order to assess the impact of water quality variations on the recovery rate.
- A small variation in T_{LEID} might cause a large variation of any process parameter if it occurs in a certain range of Q_{CHF} and Q_{FILM} . This trend means that the repeatability of any future measurement method of T_{LEID} must be better than that of the measurement of Q_{FILM} and Q_{CHF} .
- Each of the three tested issues responsible for the diminution of the recovery rate (hot tearing, bleed-out, butt curl) can be dominantly influenced by Q_{FILM} or Q_{CHF} , which, at a certain critical value, has such a strong influence that the effect of the others becomes negligible. In this case, there is no three-way interaction between T_{LEID} , Q_{FILM} and Q_{CHF} and the variable that has an impact on the recovery rate remains almost constant regardless the value of the other boiling parameters. The term "dominant factor" has been used in this paper to define the situation. The results obtained show that Q_{CHF} is the dominant factor for the sump depth and the butt curl while Q_{FILM} is the dominant factor for the shield thickness.

ACKNOWLEDGEMENTS

This work was supported by a Postgraduate Scholarship of the Natural Sciences and Engineering Research Council of Canada (NSERC). The authors express their thanks to Messrs. Guillaume Bonneau, Patrice Paquette and Pascal Vandal at UQAC for the technical assistance they offered in the execution of the project. The first author also recognizes the support given by ALCOA Technical Centre and expresses his thanks for the possibility to use certain experimental facilities during his stay at ATC.

NOMENCLATURE

Abbreviations

ATC	Alcoa Technical Center
CPU	Central Processing Unit
DC	Direct Chills
FFZ	Free Falling Zone
FR	Experimental water flow rate
IHCP	Inverse heat conduction problem
UCD	Upstream Conduction Distance

Symbols

a	Constant used to represent the influence of thermal properties and casting temperatures inside equation 1
C_s	Specific heat of solid (J/kg·°C)
E	Thermocouple position used inside IHCP (m)
Fo^+	dimensionless Fourier number
h_{al}	Convective heat transfer coefficient between liquid aluminum and the mold (W/(°C·m ²))
h_w	Convective heat transfer coefficient of water inside the cavity of the mold (W/°C·m ²)
HCS	Hot cracking index according Clyne and Davies
H_{sump}	Sump depth (m)
k_{mold}	Casting mold heat conductivity (W/(°C·m))
k_s	Thermal conductivity of solid W/(°C·m))
L_w	Wall thickness (m)
Q_{film}	Film boiling heat flux (W/m ²)
Q_{chf}	Critical heat flux (W/m ²)
R	Billet radius or Ingot thickness for rolling ingot (m)
$T_{0.3m}$	Temperature at 0.3 m withdrawal length (°C)
T_{base}	Ingot base temperature at the middle of the ingot lip (°C)
T_{chf}	Surface temperature at the critical heat flux (°C)
T_{IMP}	Surface temperature of the ingot at the impingement zone (°C)
T_{leid}	Leidenfrost temperature (°C)
T_{liq}	Temperature of the liquid aluminum (°C)

T_{liquidus}	Liquidus temperature ($^{\circ}\text{C}$)
T_{m}	Melting temperature ($^{\circ}\text{C}$)
T_{onb}	Temperature at the onset of nucleate boiling ($^{\circ}\text{C}$)
T_{solidus}	Solidus temperature ($^{\circ}\text{C}$)
T_{surf}	Surface temperature ($^{\circ}\text{C}$)
T_{w}	Water temperature ($^{\circ}\text{C}$)
U	Overall heat transfer coefficient ($\text{W}/(^{\circ}\text{C}\cdot\text{m}^2)$)
V_{cast}	Casting speed (m/s)
x_{mold}	Horizontal distance between the water hole and the mold surface (m)
α	Thermal diffusivity (m^2/s)
ΔH_{f}	Latent heat of fusion (J/kg)
Δt	time step used inside IHCP (sec)
ρ_{s}	Density of solid (kg/m^3)

Subscripts

max	Maximum measured value for each boiling parameter ($Q_{\text{chf}}, T_{\text{chf}}, T_{\text{leid}}, Q_{\text{film}}$)
min	Minimum measured for each boiling parameter ($Q_{\text{chf}}, T_{\text{chf}}, T_{\text{leid}}, Q_{\text{film}}$)

REFERENCES

- [1] D.G. Eskin, *Physical Metallurgy of Direct Chill Casting of Aluminum Alloys*, CRC Press, New York, 2008, pp. 1-17.
- [2] J.F. Grandfield, D.G. Eskin, I.F. Bainbridge, *Direct-Chill Casting of Light Alloys: Science and Technology*, Wiley, New Jersey, 2013, pp. 331-381.
- [3] B. Rinderer, J.F. Grandfield, *Cast house 2009 in review*, *Light Met. Age* 68 (2010) 47-49.
- [4] J. Sengupta, *Mathematical Modeling of the Evolution of Thermal Field During Start-Up Phase of the Direct Chill Casting Process for AA5182 Sheet Ingots*, PhD Thesis, University of British Columbia, Vancouver (2002).
- [5] E.K. Jensen, *Mathematical Model Calculations in Level Pour D.C. Casting of Aluminum Extrusion Ingots*, *Light Met.* 1980, *Proc. Int. Symp.* (1980) 631-642.
- [6] J.F. Grandfield and P.T. McGlade, *DC casting of aluminium: Process behaviour and technology*, *Mater. Forum* 20 (1996) 29-51.
- [7] S. Nukiyama, *Maximum and Minimum Values of Heat Transmitted from Metal to Boiling Water Under Atmospheric Pressure*, *J. Jpn. Soc. Mech. Eng.* 37 (1934) 367-374.
- [8] D.A. Peel and A.E. Pengelly, *Heat-transfer, solidification and metallurgical structure in the continuous casting of aluminum*, *ISI publication* 123 (1970) 186-196.
- [9] D. C. Weckman and P. Niessen, *A Numerical Simulation of the D.C. Continuous Casting Process including Nucleate Boiling Heat Transfer*, *Metall. Trans. B* 13 (1982) 593-602.
- [10] J.A. Bakken and T. Bergstrom, *Heat Transfer Measurements during DC Casting of Aluminium. Part I: Measurement Technique*, *Light Metals* (1986) 883-889.

- [11] J. Sengupta, D. Maijer, M.A. Wells, S.L. Cockcroft, A. Larouche, Mathematical modelling of water ejection and water incursion during the start-up phase of the dc casting process, *Light Met.* 2003, Proc. Int. Symp. (2003) 841-847.
- [12] L.I. Kiss and V. Dassyva-Raymond, A. Larouche, Identification of the different boiling regime during the quenching of a cylindrical Probe, *Alum.* 2006, Proc. Int. Symp. (2006) 201-210.
- [13] A. Larouche, J. Langlais, T. Bourgeois, A. Gendron, An integrated approach to measuring dc casting water quenching ability, *Light Met.* 1999, Proc. Int. Symp (1999) 235-245.
- [14] J. Langlais, T. Bourgeois, Y. Caron, G. Belan, D. Bernard, Measuring the heat extraction capacity of DC casting cooling water, *Light Met.* 1995, Proc. Int. Symp. (1995) 979-986.
- [15] L. I. Kiss, T. Meenken, A. Charette, Y. Lefebvre, R. Levesque, Experimental study of the heat transfer along the surface of a water-film cooled ingot, *Light Met.* 2002, Proc. Int. Symp. (2002) 981-985.
- [16] L. I. Kiss, T. Meenken, A. Charette, Y. Lefebvre, R. Levesque, Effect of water quality and water type on the heat transfer in DC casting, *Light Met.* 2003, Proc. Int. Symp. (2003) 829-834.
- [17] L.I. Kiss, S. Poncsak, S. Bolduc, B.R. Henriksen, Mechanism of the film-impingement cooling in DC casting, *Light Met.* 2007, Proc. Int. Symp. (2007) 709-714.
- [18] H. Yu, An experimental heat flux measurement of the Wagstaff water hole mold, *Light Met.* 2005, Proc. Int. Symp. (2005) 983-988.
- [19] M.A. Wells. D. Li, S.L. Cockcroft, Influence of surface morphology, water flow rate, and sample thermal history on the boiling-water heat transfer during direct-chill casting of commercial aluminum alloys, *Metall. Mater. Trans. B* 32 (2001) 929-939.
- [20] E. Caron. E, Secondary cooling in the direct-chill casting of light metals, PhD Thesis, University of British Columbia, Vancouver (2008).
- [21] D. Li, Boiling water heat transfer study during DC casting of aluminum alloys, Master Thesis, University of British Columbia, Vancouver (1999).
- [22] H. Robidou, H. Auracher, P. Gardin, M. Lebouche, L. Bogdanic, Local heat transfer from a hot plate to a water jet, *Heat Mass Transfer* 39 (2003) 861-867.
- [23] S. Bolduc, H. Yu, L.I. Kiss, A simplified method to characterize mold cooling heat transfer and an experimental study of impacts of water temperature on ingot casting, *Light Met.* 2009, Proc. Int. Symp. (2009) 863-869.
- [24] D.H. Wolf, F.P. Incropera, R. Viskanta, Jet Impingement Boiling, *Adv. Heat Transfer* 23 (1993) 1-132.
- [25] J. Sengupta, S.L. Cockcroft, D.M. Maijer, A. Larouche, Quantification of temperature, stress, and strain fields during the start-up phase of direct chill casting process by using a 3D fully coupled thermal and stress model for AA5182 ingots, *J. Mater. Sci. Eng.* 397 (2005) 157-177.
- [26] H. R. Busby and D.M. Trujillo, Numerical Solution to a Two-Dimensional Inverse Heat Conduction Problem, *International Journal for Numerical Methods in Engineering* 21 (1985) 349-359.
- [27] J. V. Beck, B. Blackwell, C.R. St-Clair, Inverse heat conduction Ill posed problems, Michigan, 1985, 309 p.
- [28] T.W. Clyne and G.J. Davies, Comparison between experimental data and theoretical predictions relating to dependence of solidification cracking on composition. *Solidif. Cast. Met., Proc. Int. Conf. Solidif.* (1979) 275-278.
- [29] E. Niyama, Some considerations on internal cracks in continuously cast steel, Japan-US Joint Seminar on Solidification of Metals and Alloys Tokyo (1977) 271-282.
- [30] M. Rappaz, J.M. Drezet, M. Gremaud, A new hot-tearing criterion, *Metall. Mater. Trans. A* 30 (1999) 449-455.

- [31] Q. Han, S. Viswanathan, D.L. Spainhower, S.K. Das, Q. Han, Nature and formation of surface cracks in DC cast ingots, *Light Met.* 2002, Proc. Int. Symp. (2002) 975-979.
- [32] N. B. Bryson, Increasing the Productivity of Aluminum DC Casting, *Light Met.* 1972, Proc. Int. Symp. (1972) 429.
- [33] W. Schneider and E.K. Jensen, Investigations about starting cracks in DC casting of 6063 type billets. Part I: Experimental results, *Light Met.* 1990, Proc. Int. Symp. (1990) 931-936.
- [34] I.I. Novikov: *Goryachelomkost tsvetnykh metallov i splavov* (Hot shortness of non-ferrous metals and alloys), Nauka, Moscow (1966).
- [35] S. Benum, D. Mortensen, H. Fjær, H.-G. Øverlie, O. Reiso, On the mechanism of surface cracking in DC cast 7xxx and 6xxx extrusion ingot alloys, *Light Met.* 2002, Proc. Int. Symp. (2002) 967-974.
- [36] B. Magnin, L. Maenner, L. Katgerman, and S. Engler, Ductility and rheology of an Al-4.5%Cu alloy from room temperature to coherency temperature, *Mater. Sci. Forum* 217–222 (1996) 1209–1214.
- [37] N.N. Prokhorov, Resistance to hot tearing of cast metals during solidification, *Russ. Castings Production* 2 (1962) 172–175.
- [38] M. Sistaninia, A.B. Phillion, J.-M. Drezet, M. Rappaz, Three-dimensional granular model of semi-solid metallic alloys undergoing solidification: Fluid flow and localization of feeding, *Acta Mater.* 60 (2012) 3902–3911.
- [39] J.F. Grandfield and L. Wang, Application of mathematical models to optimization of cast start practice for DC cast extrusion billets, *Light Met.* 2004, Proc. Int. Symp. (2004) 685-690.
- [40] G.P. Grealy, J.L. Davis, E.K. Jensens, P.A. Tondel, J. Moritz, Advances for DC ingot casting : Part 2 - heat transfer and casting results," *Light Met.* 2001 Proc. Int. Symp. (2001) 672-680.
- [41] W. Boender, A. Burghardt, E.P. Van Klaveren, J Rabenberg, Numerical simulation of DC casting; interpreting the results of thermo-mechanical model, *Light Met.* 2004 Proc. Int. Symp. (2004) 679-684.
- [42] J.B. Wiskel, Thermal Analysis of the Startup Phase for D.C. Casting of an AA5182 Aluminum Ingot, PhD Thesis, University of British Columbia, Vancouver (1995).
- [43] N. Ishikawa, Thermo-inelastic simulation of butt curl phenomena during aluminum DC casting, *Light Met.* 2005 Proc. Int. Symp. (2005) 1045-1050.
- [44] J. Sengupta, D. Maijer, M.A. Wells, S.L. Cockcroft, A. Larouche, Mathematical modelling of the thermomechanical behavior of a 5182 aluminum ingot during the start-up phase of the DC casting process: The role of bottom block, *Light Met.* 2001 Proc. Int. Symp. (2001) 879-886.
- [45] H. Yu, D.D. Leon, A.M. Hummel, Gas enhanced controlled cooling ingot mold, US Patent 7011140B1 (2006).
- [46] H. Yu, A process to reduce DC ingot butt curl and swell, *Light Met.* 1991 Proc. Int. Symp. (1980) 23-27.
- [47] F.E. Wagstaff, Means and technique for casting metals at a controlled direct cooling rate, U.S Patent 4693298 (1987).
- [48] N.B. Bryson, Reduction of ingot bottom “Bowling and Bumping” in large sheet ingot casting, *Light Met.* 1974 Proc. Int. Symp. (1974) 587-590.
- [49] M. Lalpoor, Study of Cold Cracking during DC-casting of High Strength Aluminum Alloys, PhD thesis, Delft University of Technology in the Netherlands (2010).
- [50] D.C. Weckman and P. Niessen, Mathematical models of the D.C. continuous casting process, *Can. Metall. Q.* 23 (1984) 209-216.
- [51] J.M. Drezet, M. Rappaz, Modeling of Ingot Distortions During Direct Chill Casting of Aluminum Alloys, *Metallurgical and materials transactions A* 27A (1996) 3214-3225.

- [52] M. Lalpoor, D.G. Eskin, L. Katgerman, Cold cracking development in AA7050 Direct Chill Cast Billet under various casting conditions, Metallurgical and materials transactions A 41A (2010) 2425-2434.
- [53] W. Roth, Ober die Abkühlung des Stranges beim Wasserguß, Aluminium 25 (1943) 283-291.
- [54] V.I. Dobatkin, Continuous casting and casting properties of alloys, Moscow: Oborongiz, 1948.
- [55] J.-M. Drezet, M. Rappaz, B. Carrupt, M. Plata, Experimental Investigation of Thermomechanical Effects during Direct Chill and Electromagnetic Casting of Aluminum Alloys, Metallurgical and materials transaction B 26B (1995) 821-829.